Необычные молекулярные облака.

- 1. Discovery of a distant molecular cloud in the extreme outer Galaxy with the Nobeyama 45-m telescope 1703.09829
- 2. THE DISCOVERY AND ORIGIN OF A VERY-HIGH VELOCITY CLOUD TOWARD M33. 1703.09730

A-ph
1703.09829

Discovery of a distant molecular cloud in the extreme outer Galaxy with the Nobeyama 45-m telescope

Mitsuhiro MATSUO,[1, 2, *] Hiroyuki NAKANISHI,[1, 3] Tetsuhiro MINAMIDANI,[2, 4] Kazufumi TORII,[2] Masao SAITO,[2, 4] Nario KUNO,[5] Tsuyoshi SAWADA,[6, 7] Tomoka TOSAKI,[8] Naoto KOBAYASHI,[9, 10] Chikako YASUI,[11] Hiroyuki MITO,[10] Takashi HASEGAWA,[12] and Akihiko HIROTA[6, 7]

We report the discovery of the molecular cloud whose kinematic distance is the largest in the Galaxy at the present moment, named G213.042+0.003, at $l = 213.^{\circ}042$ and $b = 0.^{\circ}003$ in the ^{12}CO($J = 1$–0) line using the Nobeyama 45-m telescope and a multi-beam receiver BEARS. This molecular cloud is located at the heliocentric distance of 21^{+12}_{-7} kpc and Galactocentric distance of 29^{+12}_{-7} kpc, which are estimated as the kinematic distances with the Galactic parameters obtained by Reid et al. (2014, ApJ, 783, 130). Its major and minor diameters and line width were measured to be $4.0^{+2.3}_{-1.3}$ pc, $3.0^{+1.7}_{-1.0}$ pc, and 1.5 km s^{-1}, respectively. The cloud mass was estimated to be $2.5^{+3.7}_{-1.4} \times 10^2\ M_{\odot}$ using the CO-to-H_2 conversion factor of 5.6×10^{20} cm^{-2} (K km s^{-1})$^{-1}$ obtained in far outer Galaxy.

Побудительный мотив:

В далеких областях диска SF продолжается, а CO не регистрируется .

One of the reasons why CO emission was not detected is that observations for external galaxies cannot reach enough spatial resolution and sensitivity.

No survey towards the third Galactic quadrant, where candidates of distant young stars found by Nakanishi et al. (2008), has yet been carried out.

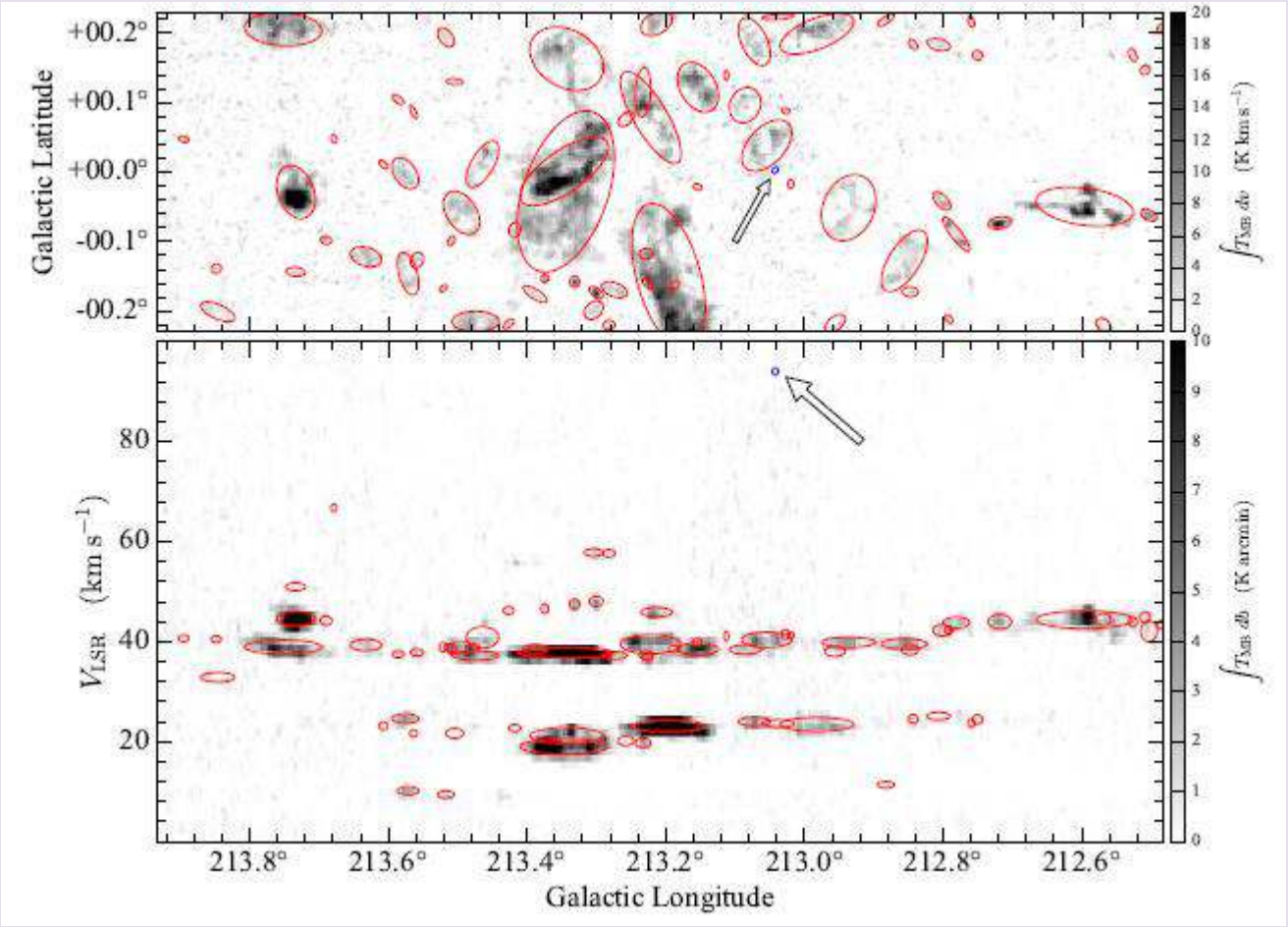

Fig. 1. Top: The Integrated intensity map obtained by integrating emission over the velocity range of 0 – 100.1 km s^{-1}. Bottom: The l-v diagram obtained by integrating the Galactic latitude range from $-0.^{\circ}25$ to $+0.^{\circ}25$. The blue denotes G213.042+0.003 and the red ellipses denote the other cloud. The arrows point to the location of G213.042+0.003.

Table 2. Physical parameters of G213.042+0.003

parameter	value
Galactocentric radius: R	29^{+12}_{-7} kpc
Distance from LSR: D	21^{+12}_{-7} kpc
Major diameter: $d_{\rm maj}$	$4.0^{+2.3}_{-1.3}$ pc
Minor diameter: $d_{\rm min}$	$3.0^{+1.7}_{-1.0}$ pc
Position angle	57.°2
Spherical radius: r^*	$1.7^{+1.0}_{-0.6}$ pc
Deconvolved radius: $r_{\rm dc}{}^{\dagger}$	$0.52^{+0.30}_{-0.17}$ pc
FWHM line width: ΔV	1.5 km s^{-1}
Peak temperature ($T_{\rm MB}$)	1.15 K
Integrated Intensity	8.6 K km s^{-}
CO luminosity: $L_{\rm CO}$	21^{+31}_{-12} K km
CO luminosity mass: $M_{\rm CO}$	$2.5^{+3.7}_{-1.4} \times 10^2$ $M_\odot$
H_2 column density: $N(H_2)$	1.2×10^{21} H_2 cm^{-2}
Virial mass: $M_{\rm VT}$	$2.2^{+1.3}_{-0.7} \times 10^2$ $M_\odot$

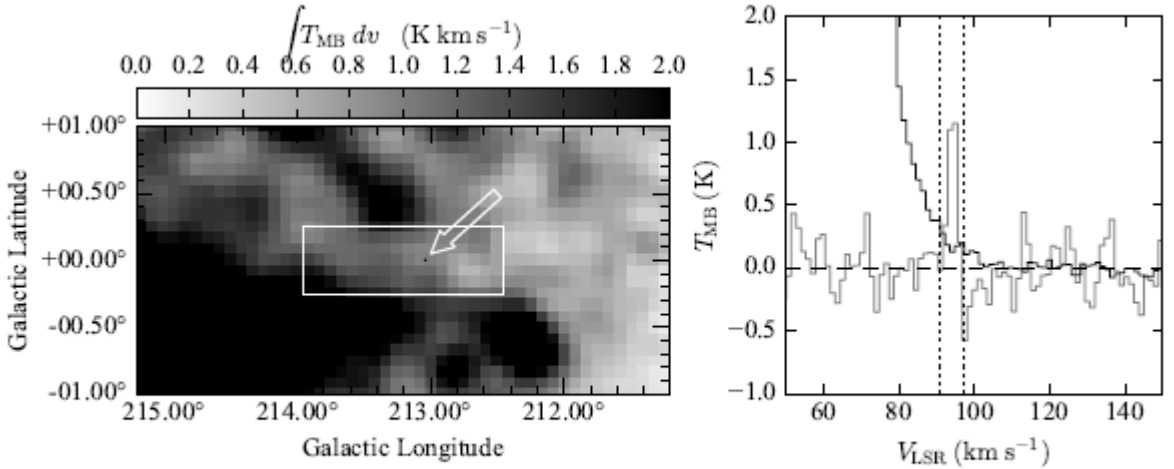

Fig. 5. Left: The Integrated intensity map of H I (HI4PI) range of 91.6 – 96.7 km s^{-1}. The white rectangle shows the observed region in this study. The ellipse shows the position and size of G213.042+0.003. The arrows point to the location of G213.042+0.003. Right: The black and gray lines are the H I and CO spectra at the position of G213.042+0.003, respectively. $T_{\rm rms}$ of H I spectrum was 0.034 K. The vertical dotted lines show the integrated velocity range of the left map.

Практически нет HI в том же интервале скоростей

$$(\Sigma_{\rm HI} < 1\,M_\odot\,{\rm pc}^{-2} \text{ and } \Sigma_{\rm H_2} < 0.1\,M_\odot\,{\rm pc}^{-2}$$

Since there is no other molecular cloud around G213.042+0.003, it seems to be an isolated molecular cloud beyond the new arm.

A-ph 1703.09730

THE DISCOVERY AND ORIGIN OF A VERY-HIGH VELOCITY CLOUD TOWARD M33

Y. Zheng[1], J. K. Werk[2],, J. E. G. Peek[3], M. E. Putman[1]

[1] Department of Astronomy, Columbia University, New York, NY 10027, USA; yzheng@astro.columbia.edu

[2] Department of Astronomy, University of Washington, Seattle, WA 98195-1580, USA

[3] Space Telescope Science Institute, 3700 San Martin Dr, Baltimore, MD 21218, USA

Abstract

We report the detection of a largely ionized very-high velocity cloud (VHVC; $v_{\rm LSR} \sim -350$ km s^{-1}) toward M33 with the *Hubble Space Telescope*/Cosmic Origin Spectrograph. The VHVC is detected in O I, C II, Si II, and Si III absorption along five sightlines separated by $\sim 0.06 - 0.4°$. On sub-degree scales, the velocities and ionic column densities of the VHVC remain relatively smooth with standard deviations of ± 14 km s^{-1} and ± 0.15 dex between the sightlines, respectively. The VHVC has a metallicity of [O I/H I]$= -0.56 \pm 0.17$ dex (Z$= 0.28 \pm 0.11$ Z$_\odot$). Despite the position-velocity proximity of the VHVC to the ionized Magellanic Stream, the VHVC's higher metallicity makes it unlikely to be associated with the Stream, highlighting the complex velocity structure of this region of sky. We investigate the VHVC's possible origin by revisiting its surrounding H I environment. We find that the VHVC may be: (1) a MW CGM cloud, (2) related to a nearby H I VHVC – Wright's Cloud, or (3) connected to M33's northern warp. Furthermore, the VHVC could be a bridge connecting Wright's Cloud and M33's northern warp, which would make it a Magellanic-like structure in the halo of M33.

Немного о HVC

- По определению, V_{LSR}>90 km/s – это HVC.
- Два типа: HI и ион.газ (по УФ абсорбциям)
- Металличность 0.1-0.3 солнечной.
- HST/COS: Найдено облако вдоль 5 близких направлений по абсорбциям O i, C ii, Si ii, and Si iii. V_{LSR} = 350 km/s.

The O I detection along S7 provides us a direct metallicity measurement for the VHVC without assuming any ionization correction. This is because O I and H I have comparable ionization potentials from their ground states, and O I is not likely to be heavily depleted onto dust (Jenkins 2009). As shown in Table 1, we find log N(O I)=14.00±0.07 cm^{-2} and log N(H I)=17.87±0.14 cm^{-2} for S7. Thus the gas-phase abundance is 12+log(O/H)=8.13±0.16. Using

Где может лежать облако?

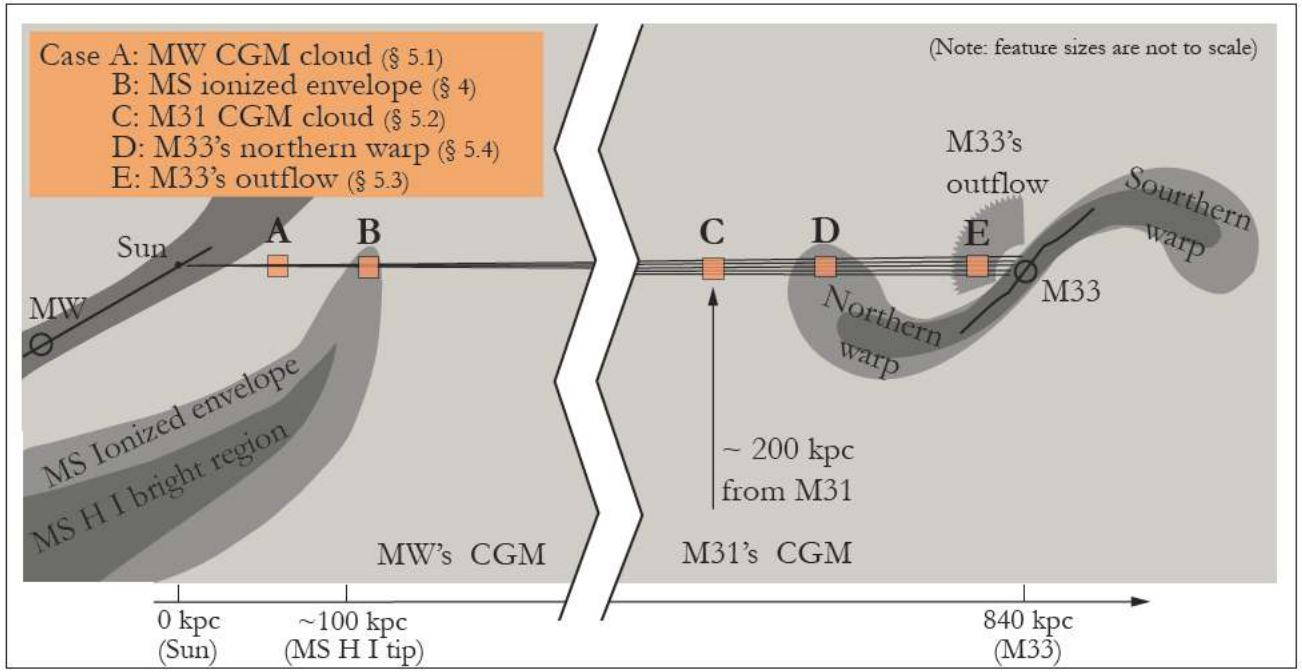

Figure 1. A cartoon showing the potential locations (A/B/C/D/E) of the VHVC along the *HST*/COS sightlines. Feature sizes are not to scale and the sizes of the orange squares at different locations are arbitrary. H I features are shown in dark gray while ionized features are indicated in light gray. We will discuss Case B – the ionized envelope of the Magellanic Stream in Section 4, and the other cases in Section 5.

Имеющиеся оценки скоростей и плотностей для данной области неба. Отмечено VHVC.

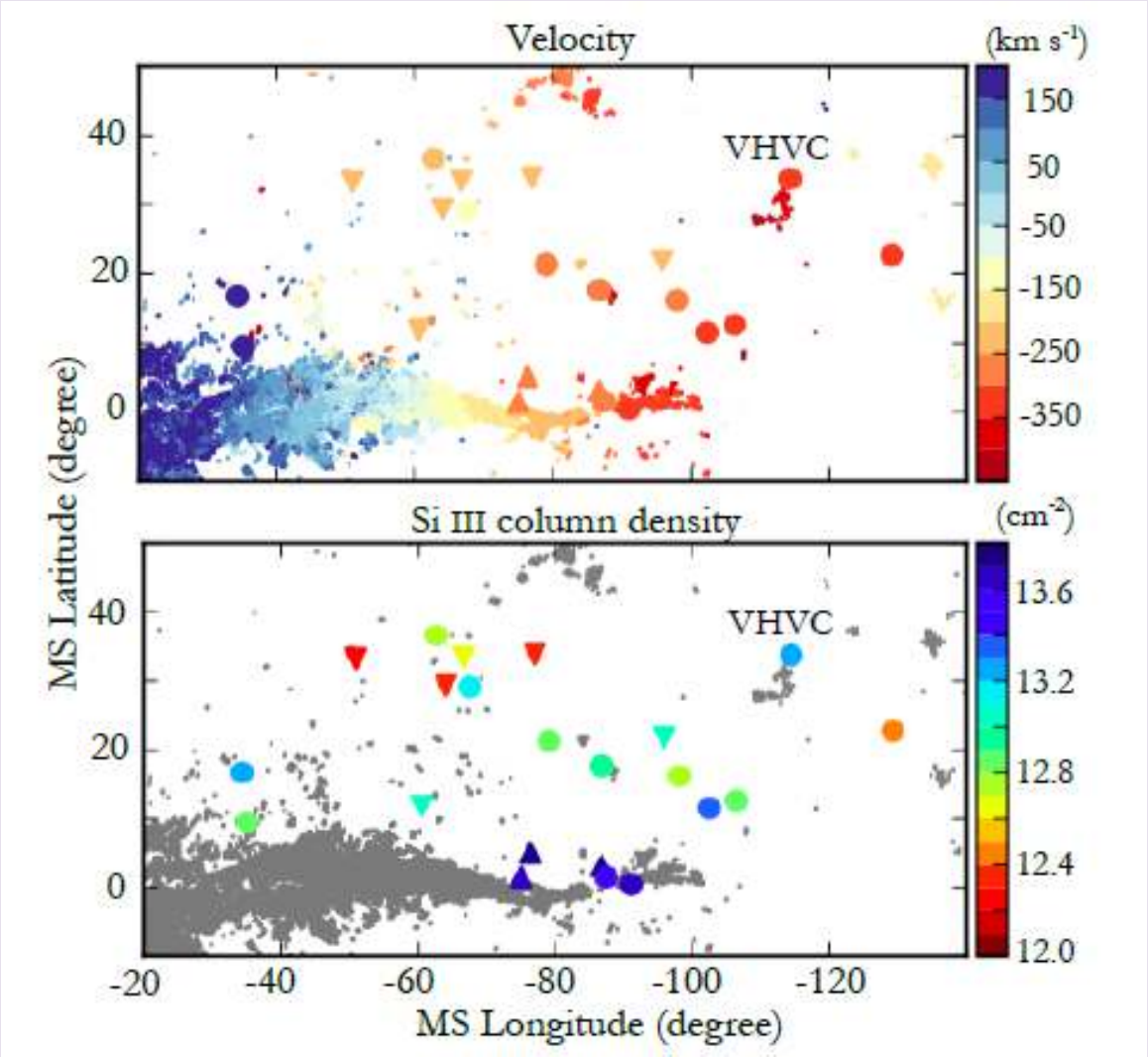

Выводы

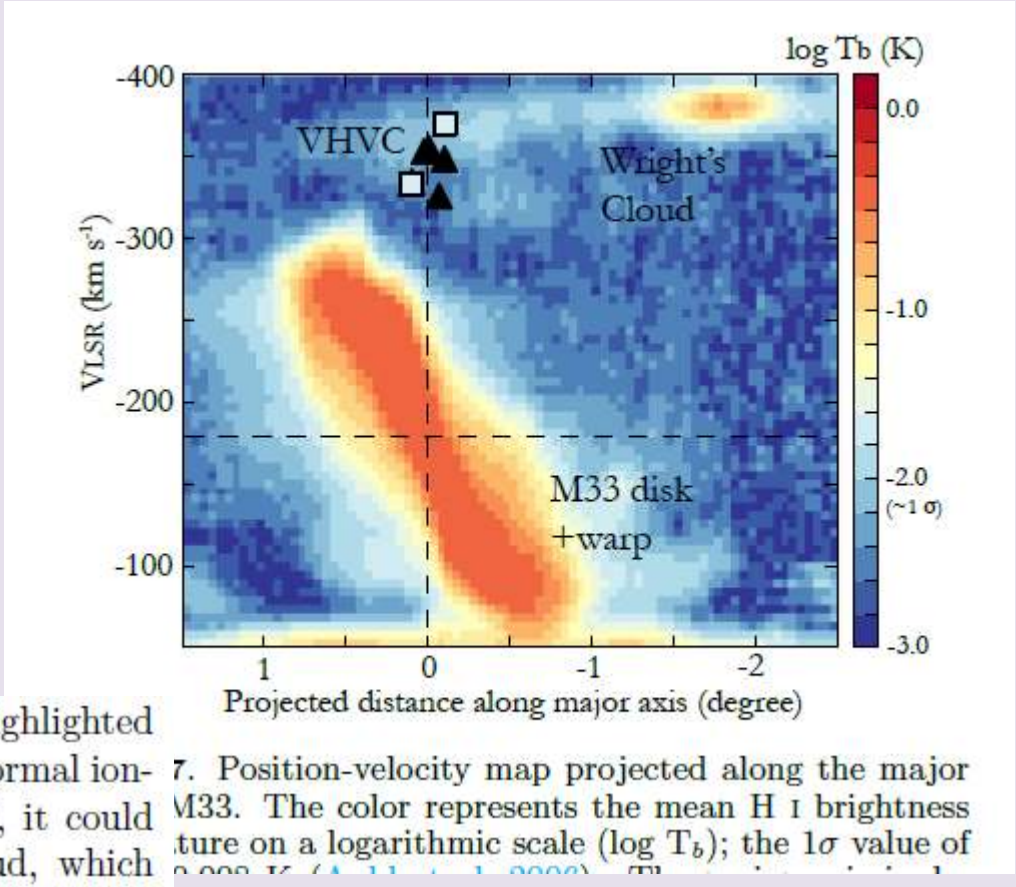

7. Position-velocity map projected along the major M33. The color represents the mean H I brightness ture on a logarithmic scale (log T_b); the 1σ value of

There remain three intriguing possibilities highlighted by our analysis. First, the VHVC could be a normal ionized absorber sitting in MW's CGM. Second, it could be associated with the nearby Wright's Cloud, which would indiate that Wright's Cloud does not belong to the Magellanic Stream. Third, it could be part of M33's northern warp given the similar metallicity and proximity in position-velocity space. If true, the data indicate that M33's northern warp is folding toward the MW. The VHVC's metallicity would imply an ISM origin for the warp, favoring the scenario that M33's warp was formed during a past interaction between M33 and M31.

HALOGAS OBSERVATIONS OF NGC 4559: ANOMALOUS AND EXTRA-PLANAR HI AND ITS RELATION TO STAR FORMATION

Carlos J. Vargas[1], George Heald[2,3,4], René A.M. Walterbos[1], Filippo Fraternali[4,5], Maria T. Patterson[6], Richard J. Rand[7], Gyula I. G. Józsa[8,9,10], Gianfranco Gentile[11], Paolo Serra[12]

[1]Department of Astronomy, New Mexico State University, Las Cruces, NM 88001

[2]CSIRO Astronomy and Space Science, 26 Dick Perry Ave, Kensington WA 6151 Australia

[3]The Netherlands Institute for Radio Astronomy (ASTRON), Dwingeloo, The Netherlands

[4]Kapteyn Astronomical Institute, University of Groningen, Postbus 800, 9700 AV Groningen, The Netherlands

[5]Dept. of Physics and Astronomy, University of Bologna, Viale Berti Pichat 6/2, 40127, Bologna, Italy

[6]Department of Astronomy, University of Washington, Box 351580, Seattle, WA 98195

[7]Department of Physics and Astronomy, University of New Mexico, 1919 Lomas Blvd. NE, Albuquerque, NM 87131

[8]SKA South Africa Radio Astronomy Research Group, 3rd Floor, The Park, Park Road, Pinelands 7405, South Africa

[9]Rhodes Centre for Radio Astronomy Techniques & Technologies, Department of Physics and Electronics, Rhodes University, PO Box 94, Grahamstown 6140, South Africa

[10]Argelander-Institut für Astronomie, Auf dem Hügel 71, D-53121 Bonn, Germany

[11]Department of Physics and Astrophysics, Vrije Universiteit Brussel, Pleinlaan 2, 1050 Brussels, Belgium

[12]INAF Osservatorio Astronomico di Cagliari, Via della Scienza 5, I-09047 Selargius (CA), Italy

ABSTRACT

We use new deep 21 cm HI observations of the moderately inclined galaxy NGC 4559 in the HALOGAS survey to investigate the properties of extra-planar gas. We use TiRiFiC to construct simulated data cubes to match the HI observations. We find that a thick disk component of scale height $\sim$ 2 kpc, characterized by a negative vertical gradient in its rotation velocity (lag) of $\sim 13 \pm 5$ km s^{-1} kpc^{-1} is an adequate fit to extra-planar gas features. The tilted ring models also present evidence for a decrease in the magnitude of the lag outside of R_{25}, and a radial inflow of ~ 10 km s^{-1}. We extracted lagging extra-planar gas through Gaussian velocity profile fitting. From both the 3D models and and extraction analyses we conclude that $\sim 10 - 20\%$ of the total HI mass is extra-planar. Most of the extra-planar gas is spatially coincident with regions of star formation in spiral arms, as traced by Hα and GALEX FUV images, so it is likely due to star formation processes driving a galactic fountain. We also find the signature of a filament of a kinematically "forbidden" HI, containing $\sim 1.4 \times 10^6$ M$_\odot$ of HI, and discuss its potential relationship to a nearby HI hole. We discover a previously undetected dwarf galaxy in HI located $\sim 0.4^\circ$ (~ 58 kpc) from the center of NGC 4559, containing $\sim 4 \times 10^5$ M$_\odot$. This dwarf has counterpart sources in SDSS with spectra typical of HII regions, and we conclude it is two merging blue compact dwarf galaxies.

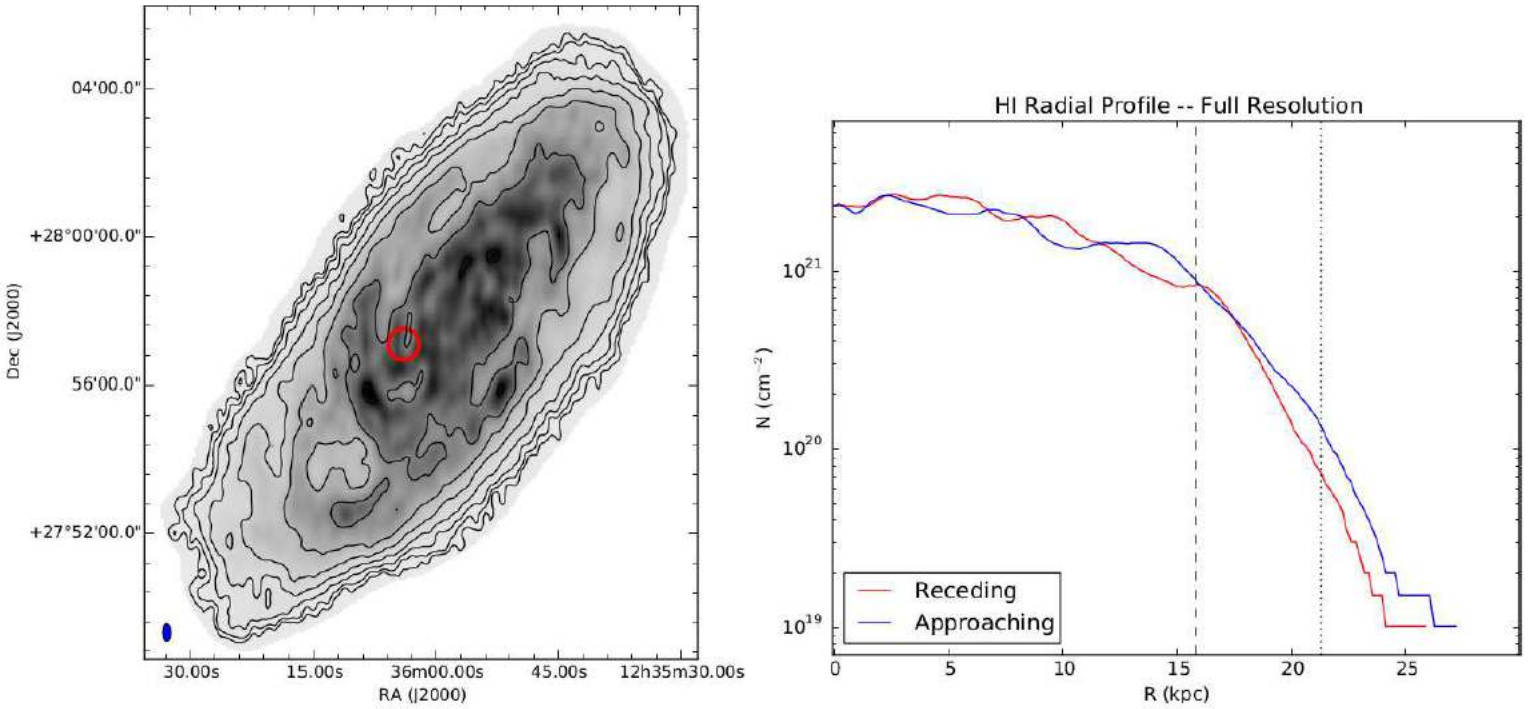

Figure 1. Left: Integrated HI map of the highest resolution HALOGAS data cube for NGC 4559. Column density contours begin at 2.4×10^{19} atoms cm^{-2} and increase in multiples of 2. The red circle marks the location of an HI hole discussed further in Section 5.2. Right: Radial profile obtained from the highest resolution integrated HI map. The vertical dashed line represents R_{25} of the galaxy, and the dotted vertical line is the largest radius at which B05 detects HI, as quoted in that text, and adjusted to our assumed distance of 7.9 Mpc.

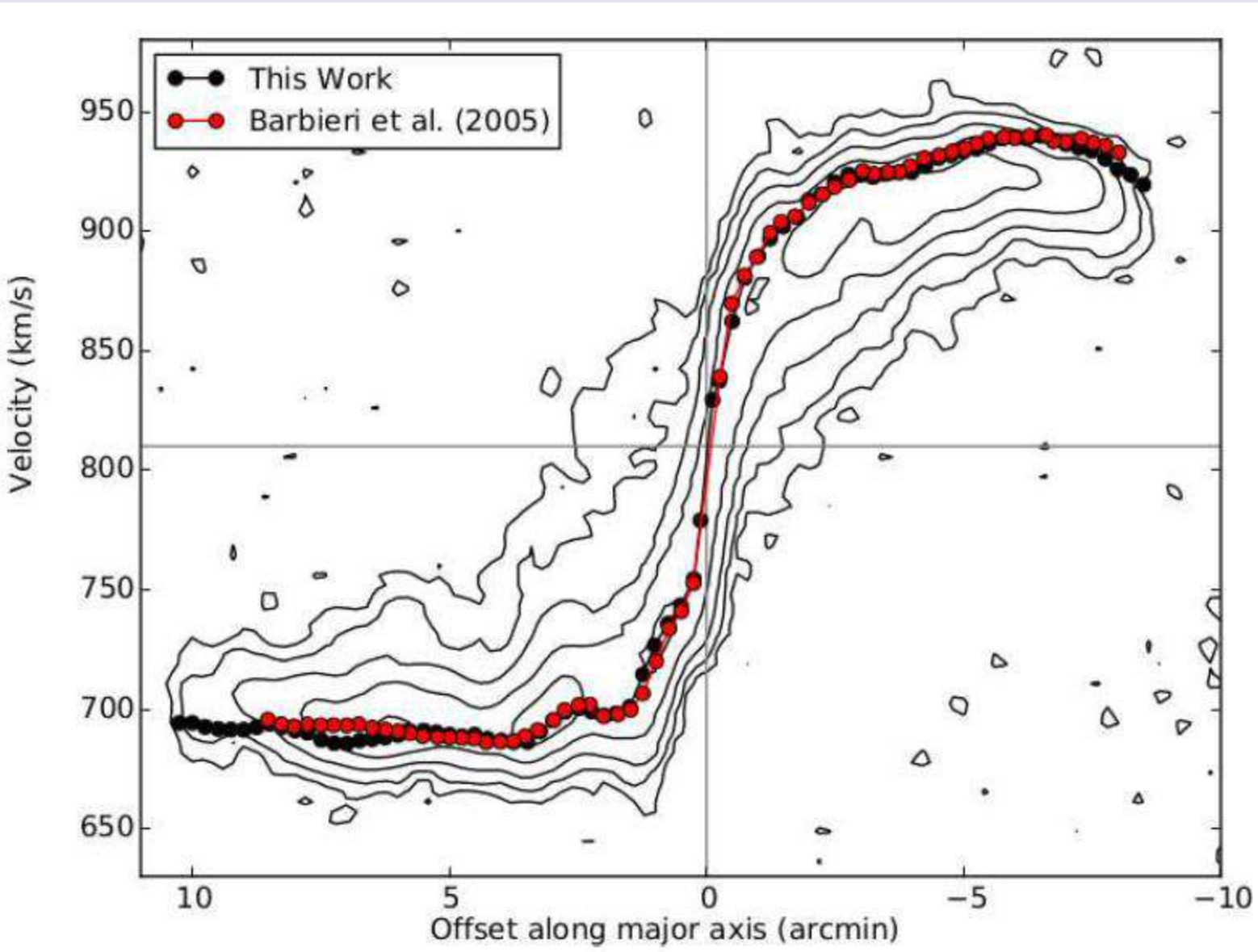
This Work
Barbieri et al. (2005)
950
900
850
800
750
700
650
Velocity (km/s)
10
5
0
−5
−10
Offset along major axis (arcmin)

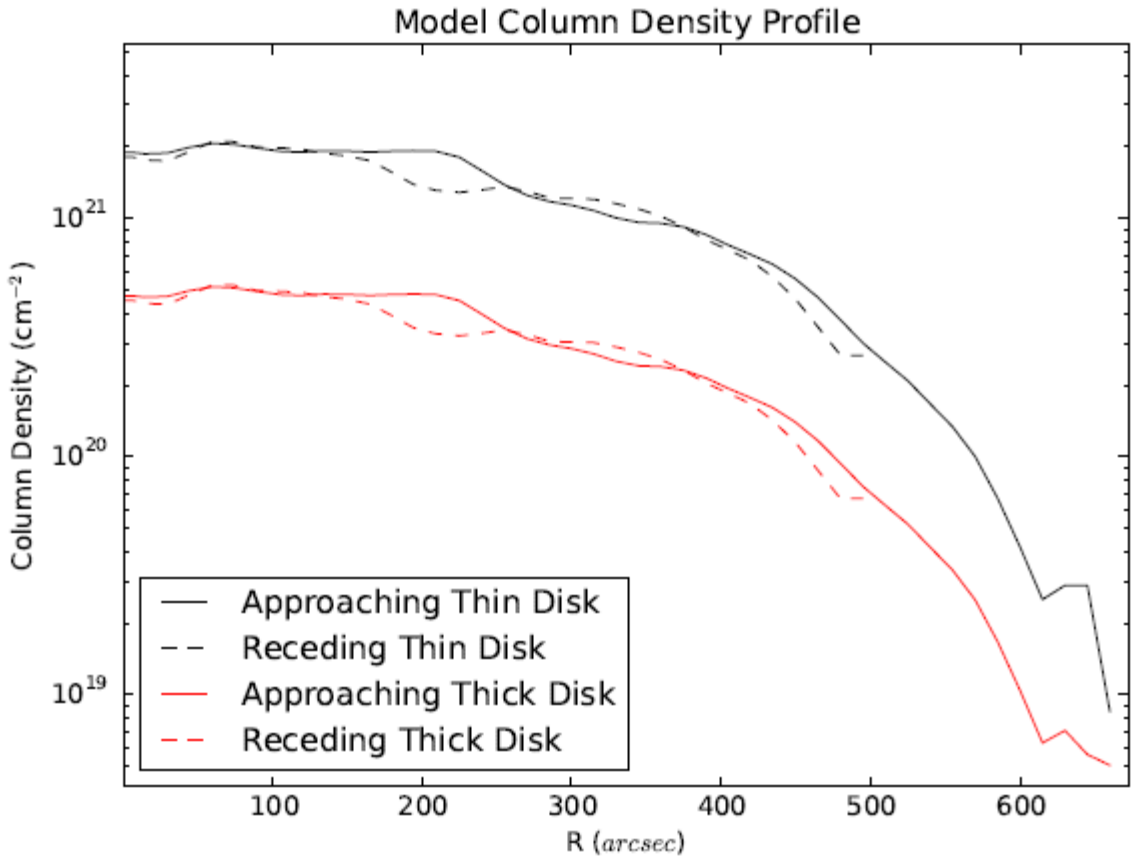

Figure 5. Column density profile for each component of the thick disk model.

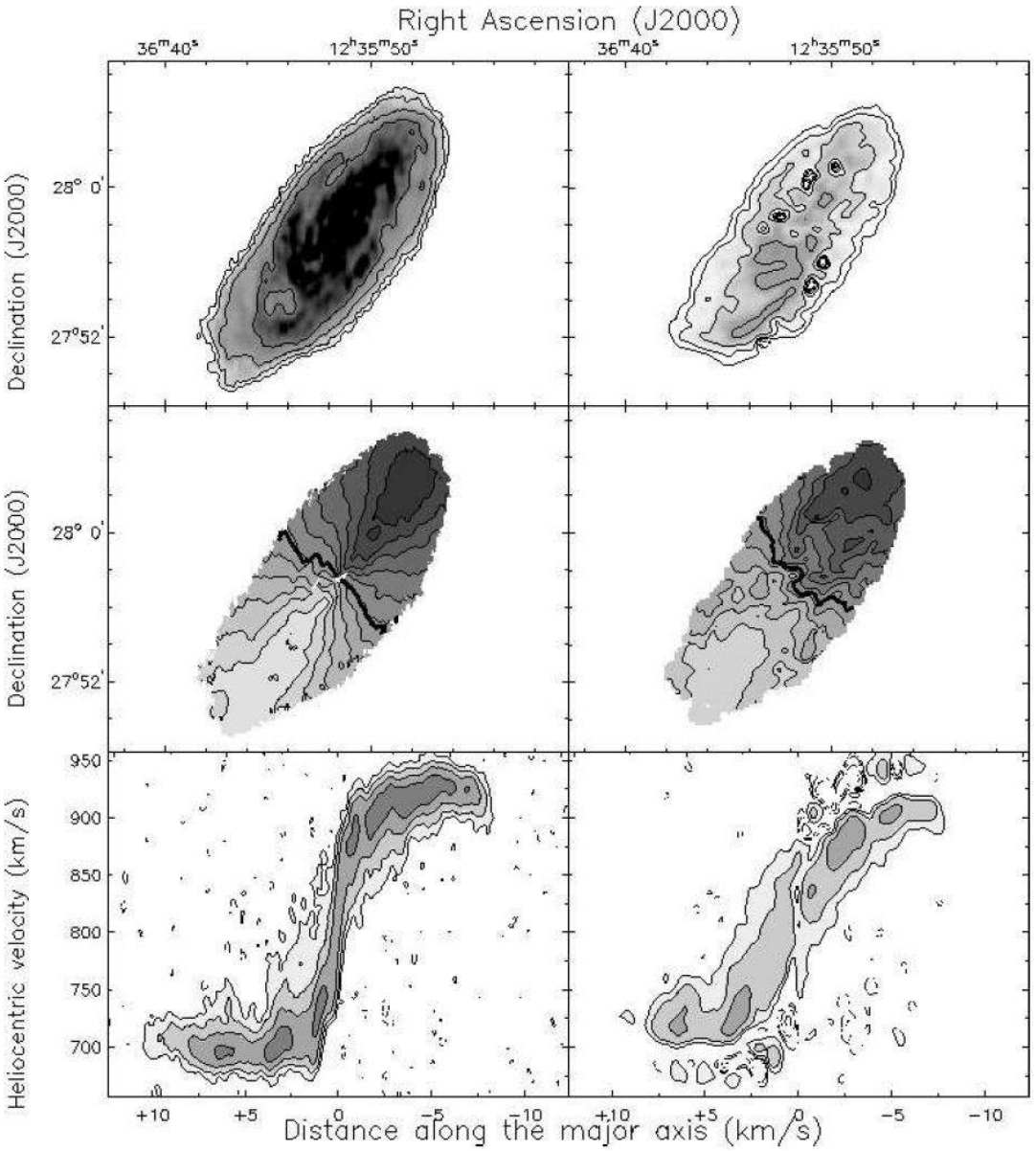

Figure 6. Various plots of the extra-planar gas extraction results. Upper left: Integrated HI map of the data, upper right: integrated HI map of the extracted extra-planar gas, middle left: velocity field of data, middle right: velocity field of extracted extra-planar gas, lower left: position-velocity slice along the major axis of the data, lower right: position-velocity slice along the major axis of the extracted extra-planar gas. All column density contours begin at 3σ in each respective cube and increase in multiples of 3. The receding half of the galaxy resides to the north-west. The velocity contours in velocity fields range 680 km s^{-1} to 940 km s^{-1} in intervals of 20 km s^{-1}. Panels in the left column are at full resolution and panels in the right column are smoothed to 30″. The upper x-axis units apply only to the top two rows, while the lower x-axis units apply to the bottom row.

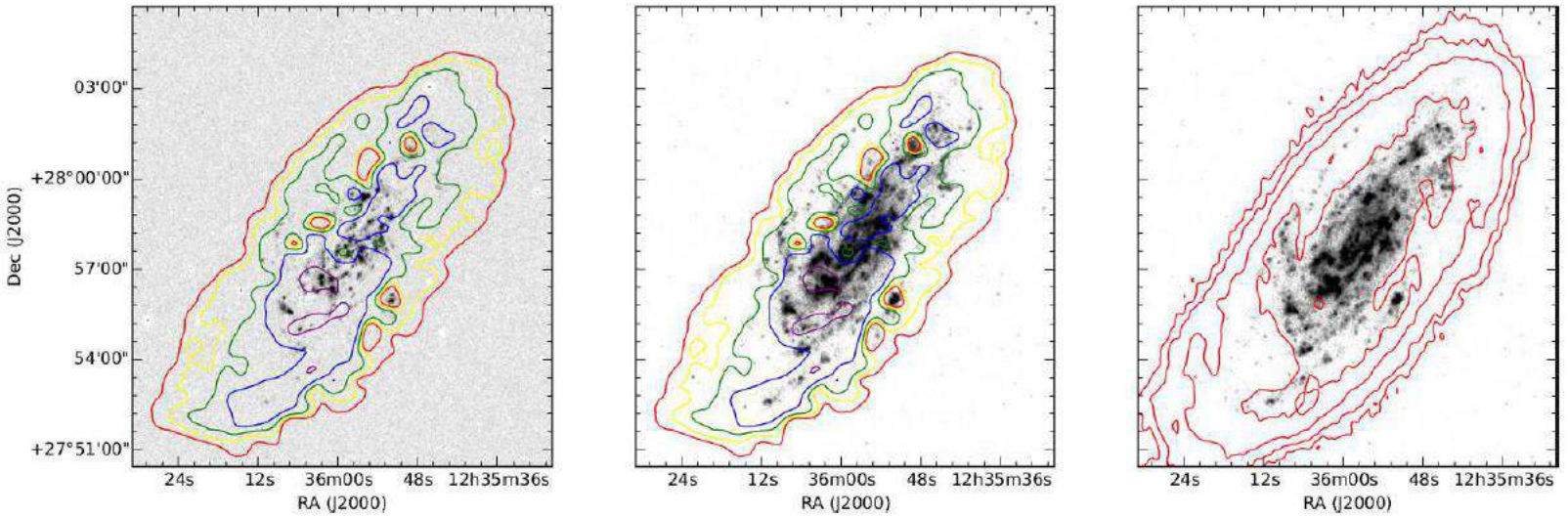

Figure 7. Left: KPNO Hα image, middle: GALEX FUV image (Gil de Paz et al. 2007), right: Galex FUV image. Overlaid atop the left two images are the total extracted extra-planar gas moment 0 contours. The colors represent different values of column density and range, from lowest to highest, red, yellow, green, blue, and violet. The contours begin at 3.75×10^{20} atoms cm^{-2} and increase in multiples of 2. Overlaid atop the rightmost image is the full resolution HI data, the same as Figure 1.

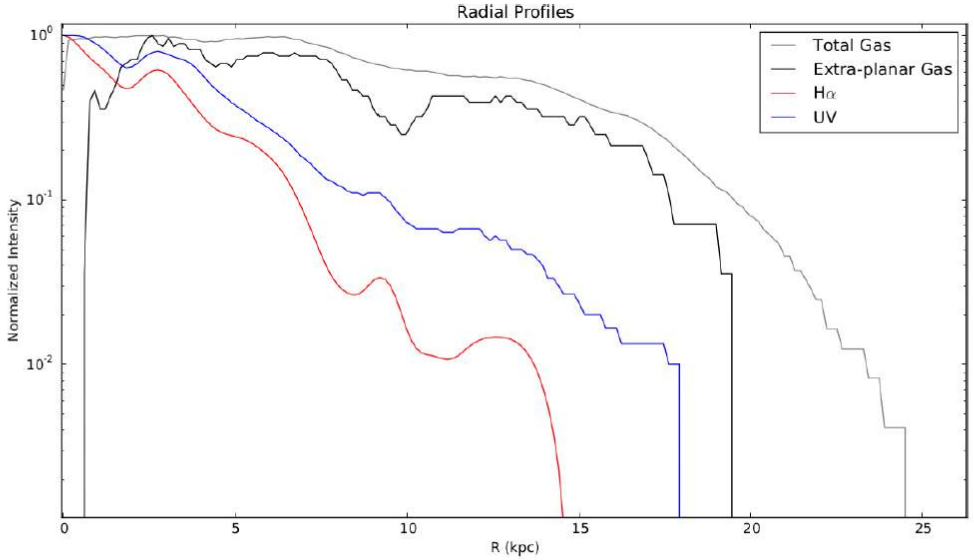

Figure 8. Radial profiles obtained from the extracted extra-planar gas, total HI map, Hα map, and GALEX UV map. The Hα and UV maps are smoothed to match the resolution of the HI map before the radial profiles are calculated. The intensities are normalized to their peak values so differences in profiles can be easily compared.

Основной вывод

We use a Gaussian line profile fitting technique to extract the anomalously rotating extra-planar gas from the normally rotating disk. In this technique we find that $\sim 10\%$ of the total H I mass is extra-planar. Also, the extra-planar gas is localized to the inner star-forming regions of the galaxy, again suggesting a bulk of this gas is of galactic fountain origin.

A-ph 1703.10301

EXTENDED IONIZED GAS CLOUDS IN THE ABELL 1367 CLUSTER [1]

MASAFUMI YAGI[2,3] MICHITOSHI YOSHIDA[4], GIUSEPPE GAVAZZI[5], YUTAKA KOMIYAMA[2,6], NOBUNARI KASHIKAWA[2,6], SADANORI OKAMURA[3,7],
yagi.masafumi@nao.ac.jp

ApJ accepted

ABSTRACT

We surveyed a central 0.6 deg^2 region of Abell 1367 cluster for extended ionized gas clouds (EIGs) using the Subaru prime-focus camera (Suprime-Cam) with a narrow-band filter that covers Hα. We discovered six new EIGs in addition to five known EIGs. We also found that the Hα tail from the blue infalling group (BIG) is extended to about 330 kpc in projected distance, which is about twice longer than previously reported. Candidates of star-forming blobs in the tail are detected. The properties of the EIG parent galaxies in Abell 1367 basically resemble those in the Coma cluster. A noticeable difference is that the number of detached EIGs is significantly fewer in Abell 1367, while the fraction of blue member galaxies is higher. The results suggest a difference in the evolutionary stage of the clusters; Abell 1367 is at an earlier stage than the Coma cluster.

Газ в скоплениях: наблюдается в рентгене, радиоконтинууме, в молекулярных линиях, и в оптических эмиссионных линиях

Extended ionized gas (EIG) – свидетельство совсем недавнего выброса из галактик. Найден в нескольких скоплениях.

ЗДЕСЬ: SUBARU.

- Abell 1367. z=0.0217. Большая доля SF-активных галактик. Не-срелаксированное скопление.
- Наблюдения SUBARU, с Ha-фильтром (2014г). Вычиталось R- изображение.

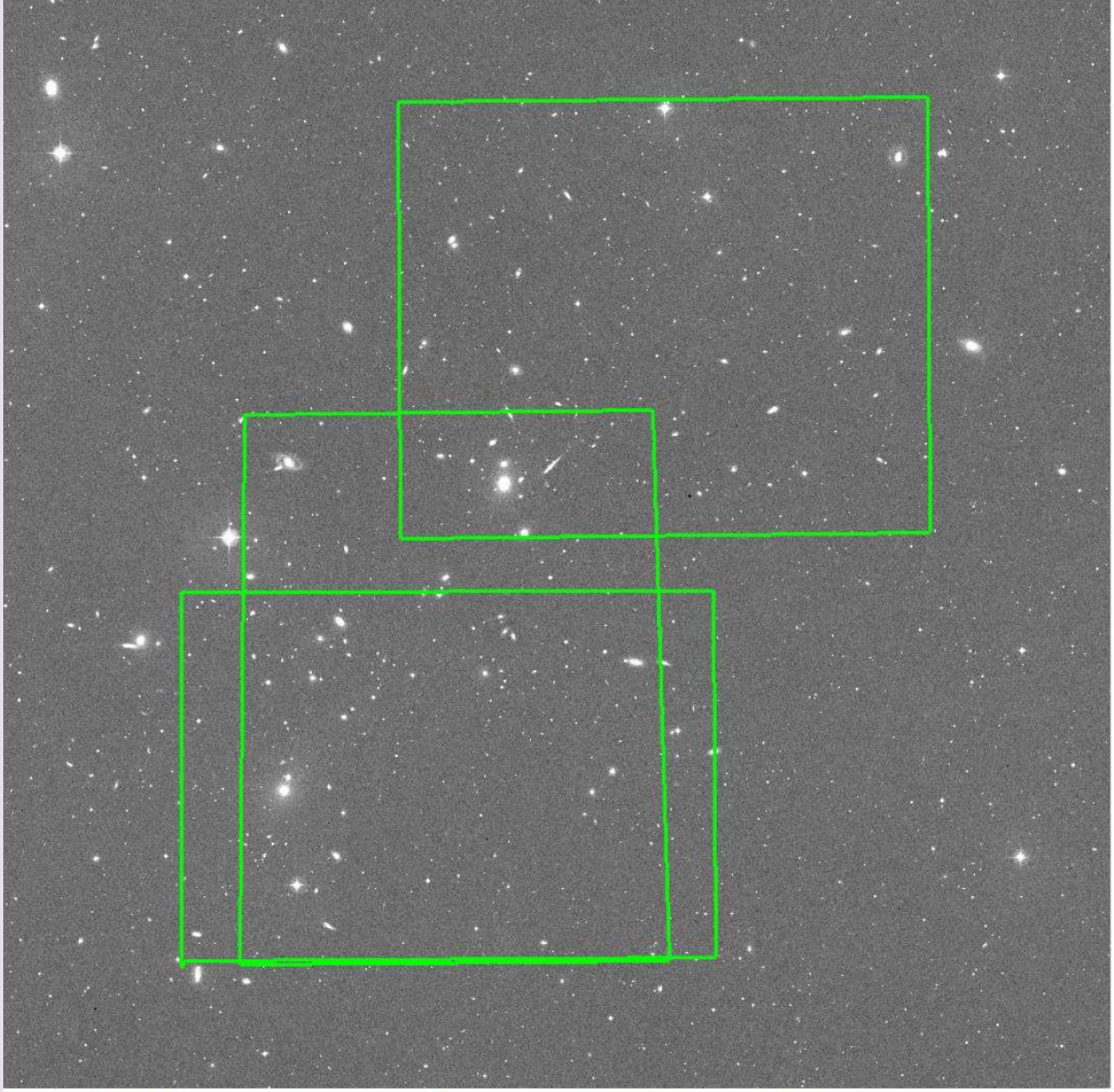

FIG. 1.— Abell 1367 cluster. The background image is R-band of Palomar Digitized Sky Survey 2 (DSS2). The size of the image is 75 arcmin square. The solid oxes represent the observed regions in this study.

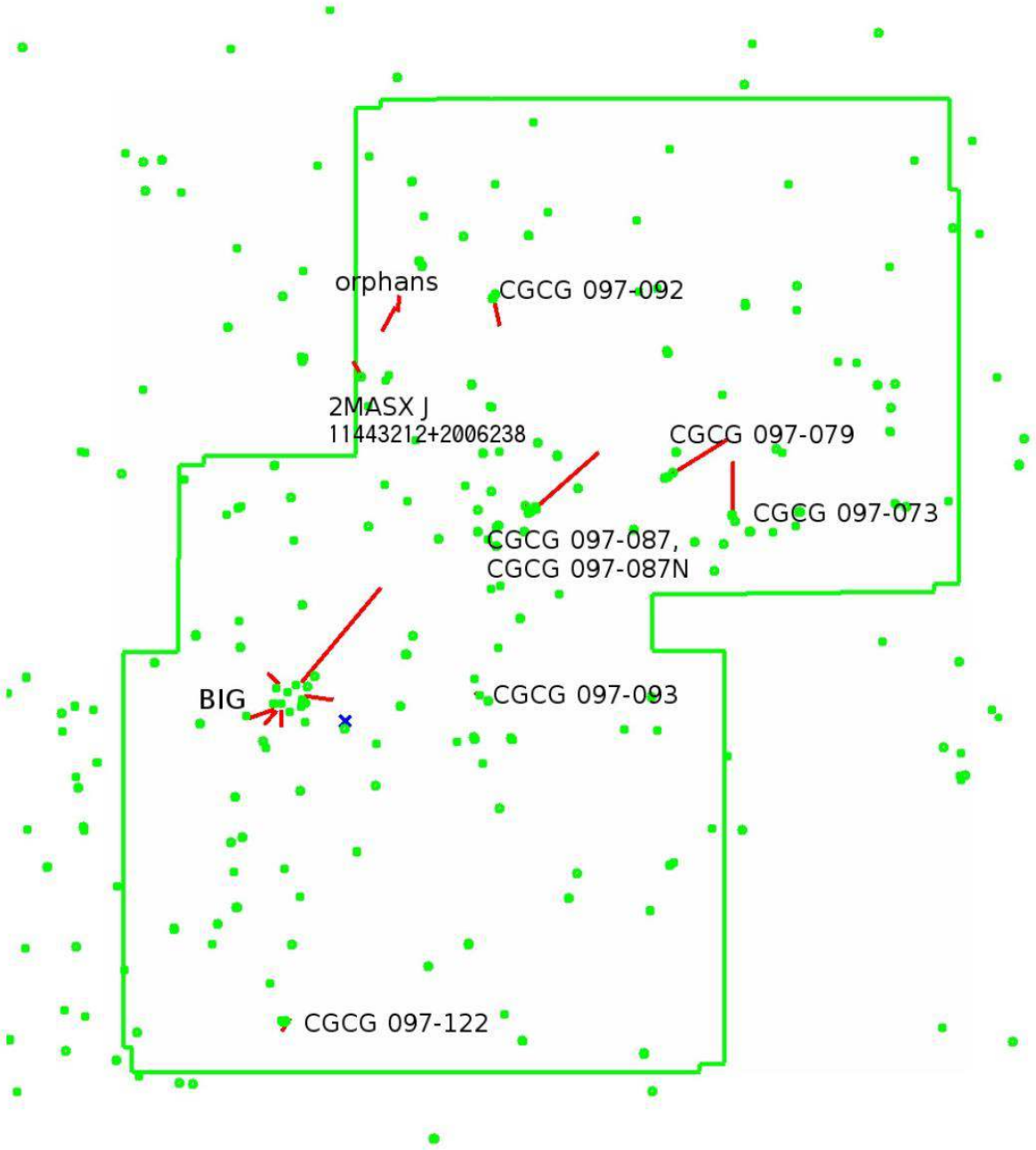

FIG. 5.— Distribution of EIGs. The green dots are spectroscopic member galaxies. The green polygon shows the observed region. The blue x-mark shows the center of the cluster (Piffaretti et al. 2011). Red lines show the major direction and length of EIGs. Each parent name is also shown. The clouds whose parents are uncertain are labeled as "orphans."

Одиночное облако

- B, I, NB-R

NB-R

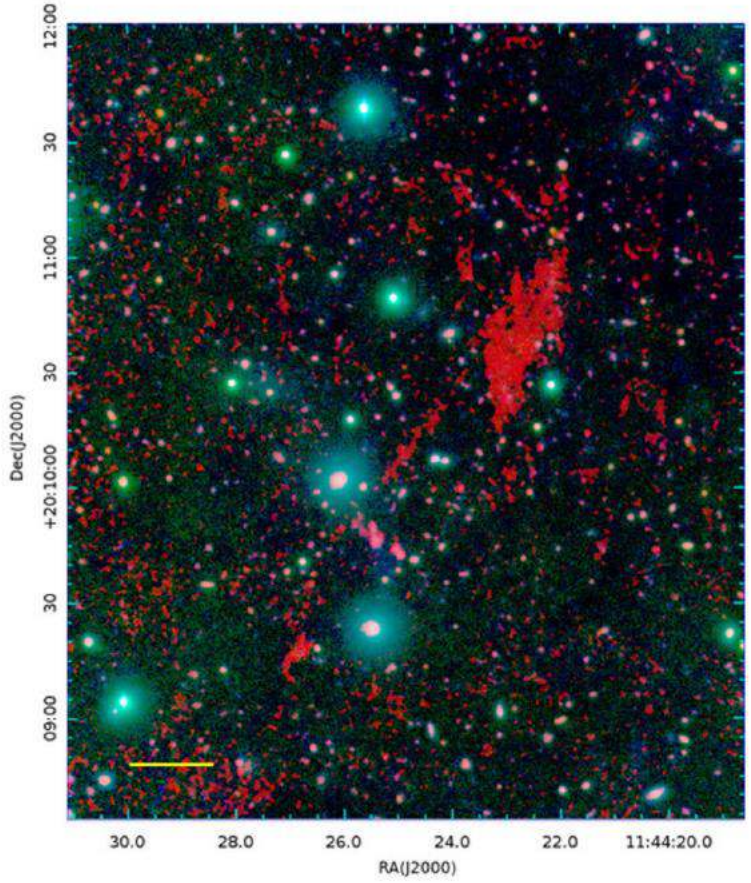

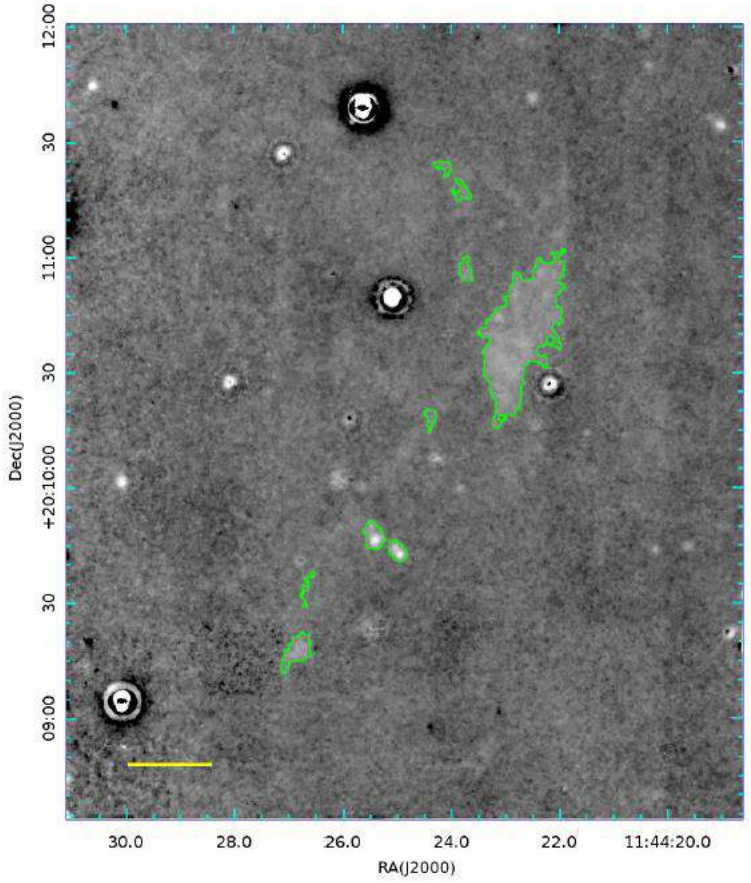

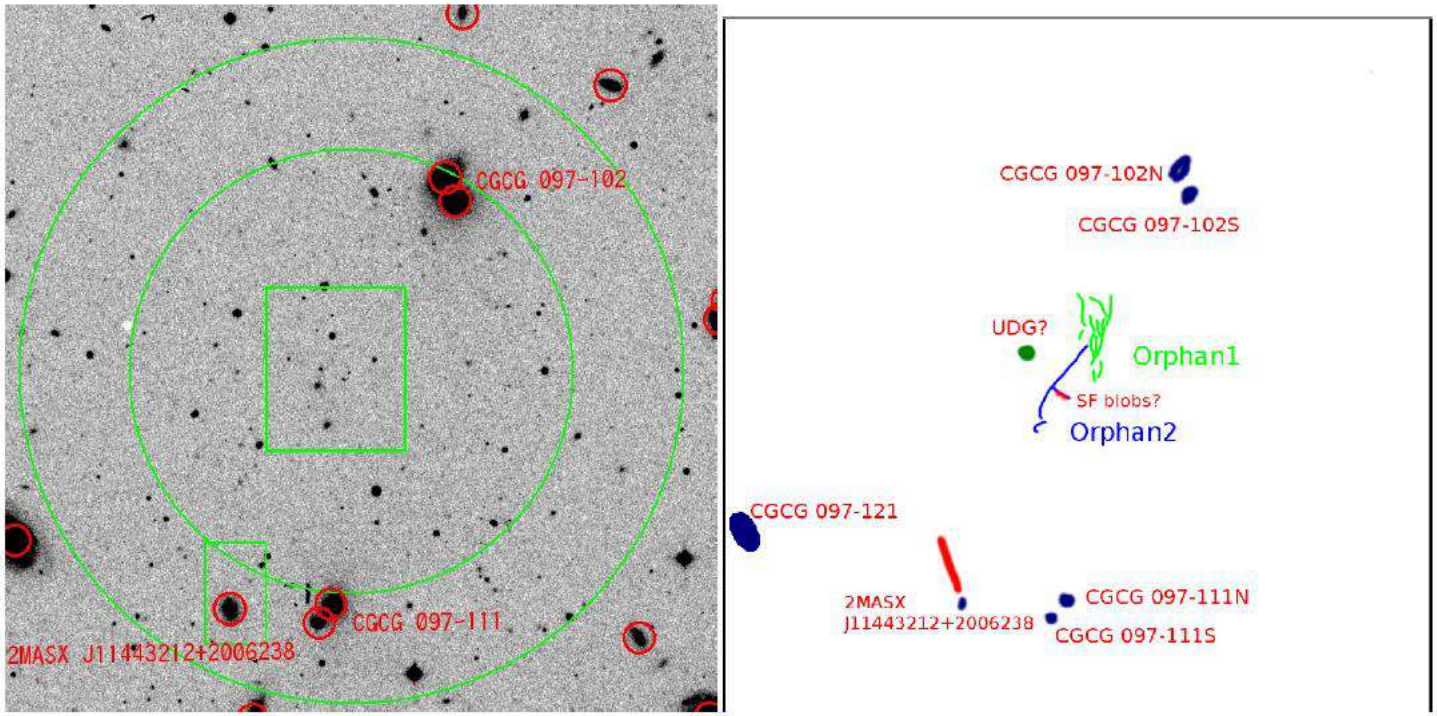

FIG. 7.— Member galaxies around the orphan clouds. (left) DSS2 image. Member galaxies are marked with red circles. The central rectangle shows the region of Figure 6, and the left-bottom box shows that of Figure 9. Two circles show scale of 100 kpc and 150 kpc from the orphan clouds. The names of member galaxies within 150kpc from the clouds are also shown. (right) Schematic figure around the clouds. The image scale is the same as the left panel. The "UDG" is not visible in top panels but is seen in Figure 6.

Проблема “Orphan clouds”

If the clouds are in Abell 1367, the size of the north clump (orphan1) is 33×20 kpc, and the south-east clump (orphan2) is 12×3 kpc. Though the isophote of 2.5×10^{-18} erg s^{-1} cm^{-2} $arcsec^{-2}$ at z=0.0217 separates the two clouds, a faint filamentary cloud is connecting the clouds and possible star-forming(SF) blobs are found between the two as seen in the left

The nearest AGN from the orphan clouds is CGCG 097-121 at $\sim$ 180 kpc in Gavazzi et al. (2011), which is classified as a LINER. If the orphan clouds are also ionized by the AGN, the ionizing flux from the AGN would be weaker by an order or more than that at Hanny's Voorwerp because of the distance. Added to that, if the ionizing flux of CGCG 097-121 is an order weaker than the source AGN of Hanny's Voorwerp, the mean surface brightness of $\sim$ 27 mag $arcsec^{-2}$ of the orphan clouds could be reproduced. Thus the AGN illumination is one of promising scenarios. Shock heating and UV from the hot gas are also promising ionizing mechanisms.

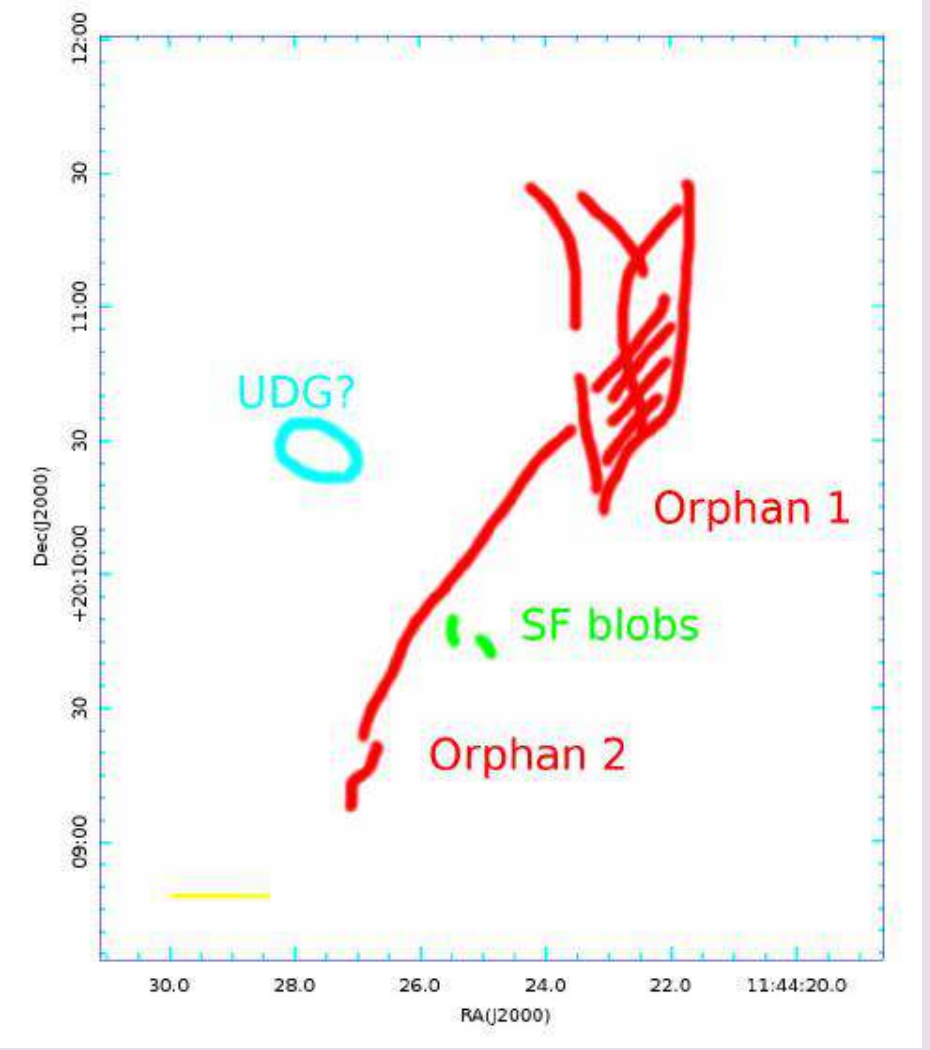

Группа «BIG» (blue infalling group)

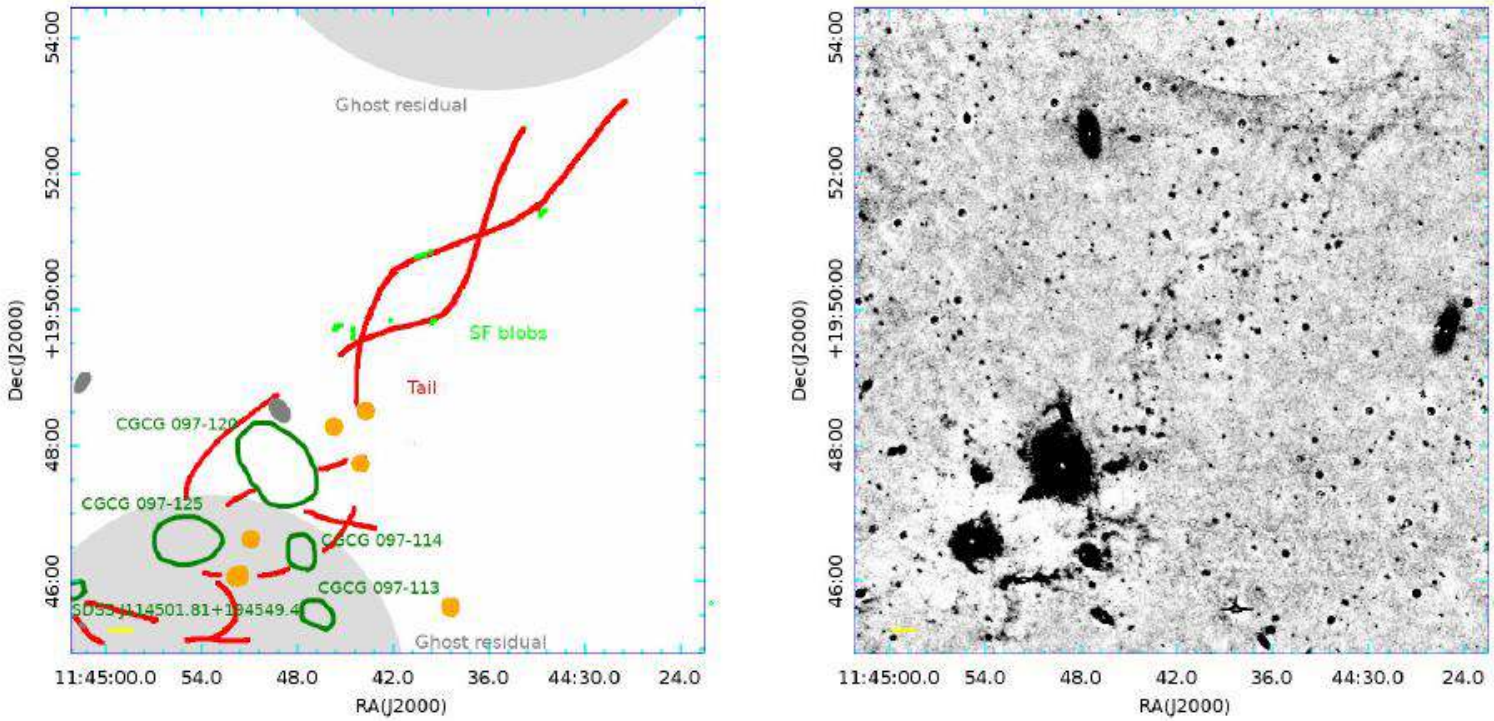

We found that the Hα tail from BIG continued about twice longer than reported by Cortese et al. (2006) reaching a projected distance of $\sim$ 330 kpc (Figure 10). The tail was called "NW" in Cortese et al. (2006).

factor. Excluding the Hα around BIG, the tail mass would be $\sim (3 \pm 2) \times 10^9 \sqrt{f_v} M_\odot$. The long tail implies that the group would have suffered the ram-pressure from the intra-cluster gas of Abell 1367 for several hundred Myrs, while the group have moved roughly straight toward the southeast.

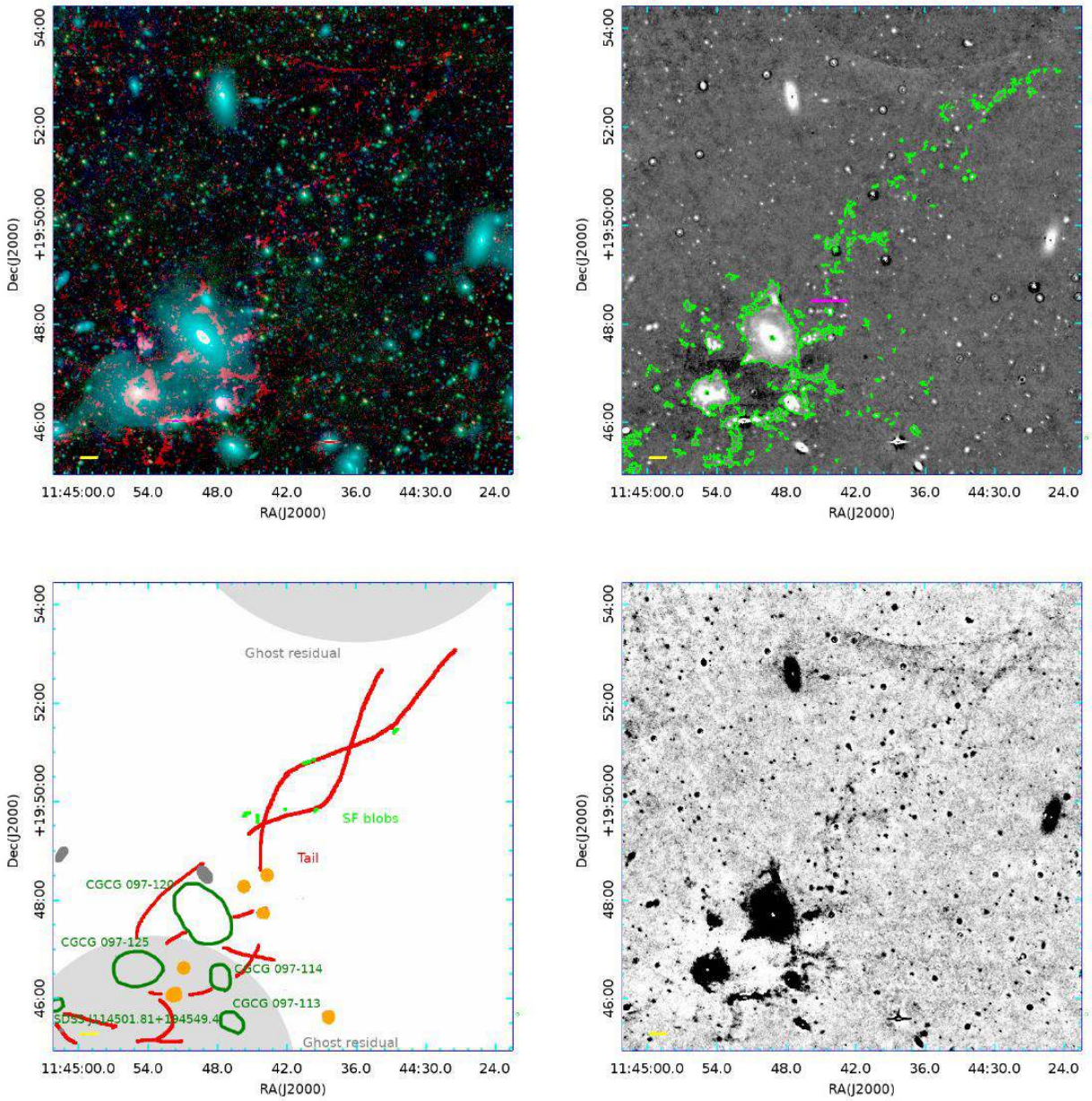

FIG. 10.— (Top panels) Same as Figure 8, but around BIG and its tail. In the top-right panel, z = 0.0275(v_r = 8244 km s^{-1}) is assumed for the green contour. Magenta line shows the adopted boundary of BIG and the tail for flux measurement. (Bottom-left) Schematic figure of BIG and tail is shown. Green ellipses are member galaxies of Abell 1367 and gray ellipses are background galaxies. Orange-filled circles are stars. Only objects near BIGs are drawn. Heavy ghost residuals are also shown as light gray circles. The possible winding streams are depicted in red. Possible SF blobs are shown in light green. (Bottom-Right) Inverted color image of Hα, with different contrast to show the morphology of the tail of BIG clearer.

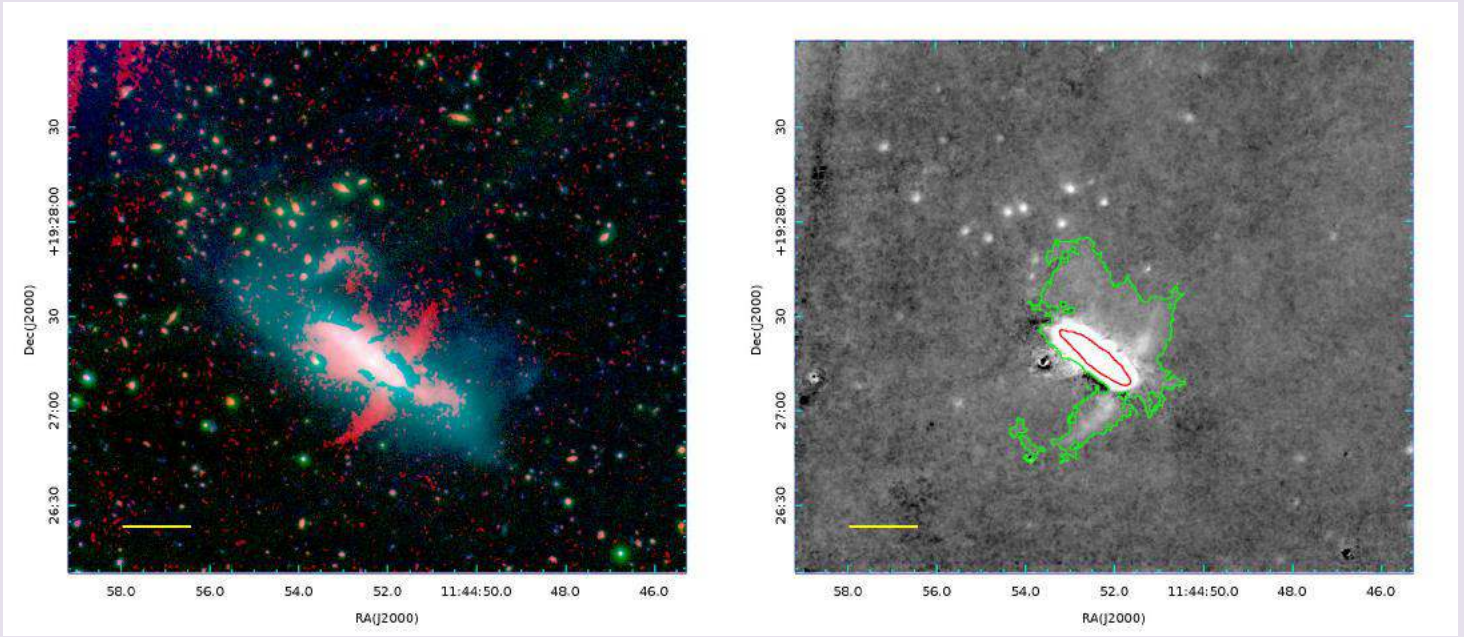

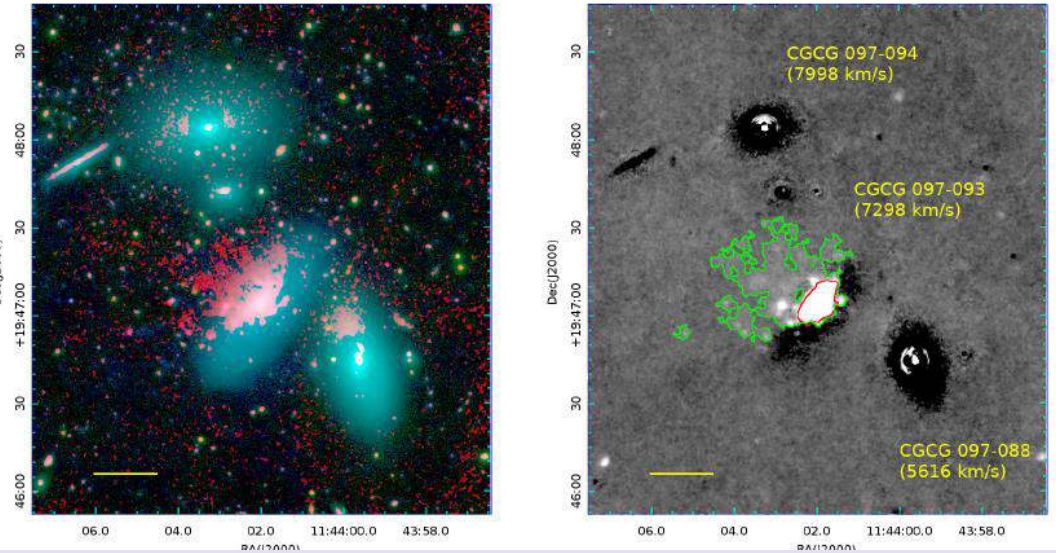

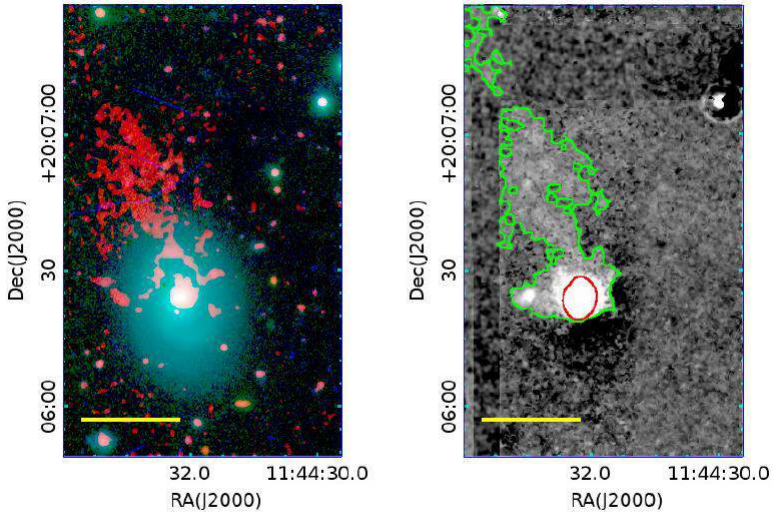

FIG. 9.— Same as Figure 8, but around 2MASX J11443212+2006238.

TABLE 2

EXTENDED Hα CLOUDS IN ABELL 1367

ID/parent (1)	size (2)	area (3)	⟨SB⟩ (4)	redshift (5)	Hα flux (6)	mass (7)	type (8)
orphan1	33×13	128	26.6±0.1	0.0217 [c]	$(3.4\pm0.2)\times10^{-15}$ [c]	$(5.4\pm0.3)\times10^{8}$ [c]	3
orphan2[d]	36×5	27	26.7±0.1	0.0217 [c]	$(4.0\pm0.2)\times10^{-16}$ [c]	$(3.1\pm0.2)\times10^{7}$ [c]	3
2MASX J11443212 +2006238	>33×13[b]	>177[b]	23.9±0.3	0.02402	$>(6\pm2)\times10^{-14}$ [b]	$>(2.8\pm0.9)\times10^{9}$ [b]	2
CGCG 097-092	35×11	91	23.2±0.3	0.02157	$(5\pm2)\times10^{-14}$	$(1.6\pm0.5)\times10^{9}$	3
(without core)	23×10	68	26.9±0.1	0.02157	$(1.4\pm0.2)\times10^{-15}$	$(2.2\pm0.3)\times10^{8}$	
CGCG 097-093	31×19	232	24.9±0.5	0.01633	$(4\pm3)\times10^{-14}$	$(3\pm2)\times10^{9}$	1
CGCG 097-122	34×28	380	23.8±0.5	0.01824	$(1.5\pm0.8)\times10^{-13}$	$(1.0\pm0.5)\times10^{10}$	1
(BIG+tail)	334×145	3306	25.0±0.5	0.0275[d]	$(5\pm3)\times10^{-13}$	$(8\pm5)\times10^{10}$	···
(tail only)	184×45	486	26.7±0.5	0.0275[d]	$(2\pm1)\times10^{-14}$	$(3\pm2)\times10^{9}$	···
CGCG 097-073	84×28	559	24.3±0.2	0.02429	$(1.3\pm0.3)\times10^{-13}$	$(1.0\pm0.2)\times10^{10}$	1
CGCG 097-079	135×17	285	23.2±0.1	0.02342	$(1.7\pm0.2)\times10^{-13}$	$(5.2\pm0.6)\times10^{10}$	1
CGCG 097-087	166×20	910	23.1±0.2	0.02218	$(5.8\pm1.1)\times10^{-13}$	$(2.3\pm0.4)\times10^{10}$	1
CGCG 097-087N	12×11	72	24.7±0.6	0.02516[a]	$(1.2\pm0.8)\times10^{-14}$	$(8\pm6)\times10^{8}$	1

(1) Name of the cloud.
(2) Size of minimum bounding rectangle of isophote of 2.5×10^{-18} erg s^{-1} cm^{-2} arcsec^{-2}. Unit is kpc×kpc.
(3) Projected area in the isophote. Unit is kpc^2.
(4) Mean surface brightness in the isophote. Unit is mag arcsec^{-2}.
(5) Redshift used for calculating Hα flux. Taken from SDSS DR12(Alam et al. 2012) unless otherwise noted.
(6) Hα flux. Unit is erg s^{-1} cm^{-2}.
(7) Mass of the cloud. Unit is $\sqrt{f_v}M_\odot$, where f_v is a volume filling factor.
(8) Morphological type (see Section 4.4.)

- Зеленые- BIG
- Красные - Hα
- Черные – осталь-

ные галактики

У Hα повышен процент голубых.

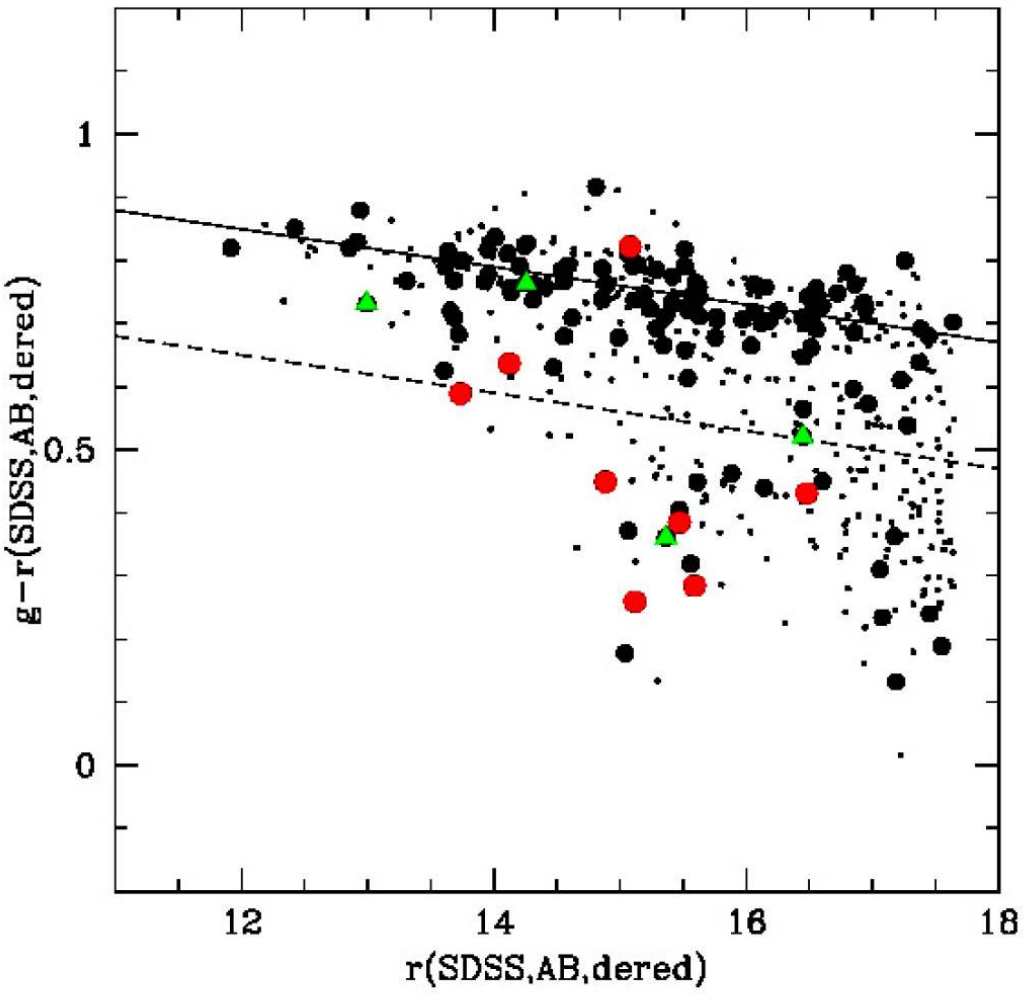

FIG. 15.— Color magnitude diagram of member galaxies of Abell 1367. The color and magnitude data are taken from SDSS DR12 except for CGCG 097-087, whose color and magnitudes are supplemented by GOLDMine Database (Gavazzi et al. 2003b), as described in the Appendix. Galaxies in the observed field and those out of the field are shown as filled circles and points, respectively. The red circles show parents of extended Hα clouds. Four BIG members (CGCG 097-120, 114, 125, and SDSS J114501.81 +194549.4) are marked by green triangles. The solid line shows color magnitude relation (CMR) of early type galaxies, and the broken line is 0.2 mag bluer than the CMR for demarcation of blue and red galaxies.

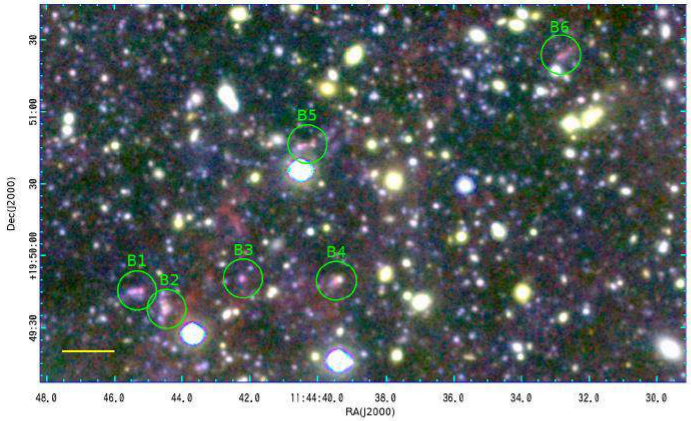

Composite

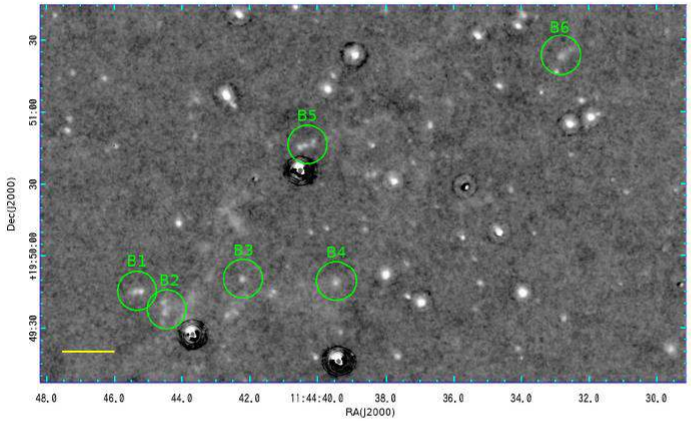

Ha

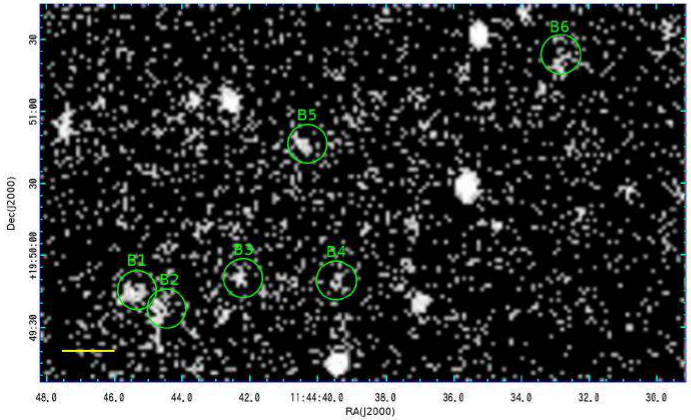

GALEX

FIG. 11.— Zoomed-up images around the SF blob candidates in the tail of BIG. Six SF blob candidates are designated as green circles. From the top to the bottom, B, R, and NBcomposite, Hα, and NUV image from GALEX archive are shown.

TABLE 5

COMA AND A1367 STATISTICS IN SURVEYED REGI

name	survey area[Mpc^2]	member	blue member	EIG parent[a]	blue parent[a]
Coma	1.2	202	15	12	8
A1367	1.7	120	19	11	6

Отсебятина.

- Время жизни EIG– не менее 10^8 лет.
- Нет явного расширения.
- Равенство давлений = на 3 порядка выше плотность. Почему низкая ME? Клочковатость?
- Эффект протуберанца = поле.

A-ph 1703.10285

ORIGIN OF NON-AXISYMMETRIC FEATURES OF VIRGO CLUSTER EARLY-TYPE DWARF GALAXIES – I. BAR FORMATION AND RECURRENT BUCKLING

SungWon Kwak[1,2], Woong-Tae Kim[1], Soo-Chang Rey[3], & Suk Kim[2]

[1]Center for the Exploration of the Origin of the Universe (CEOU), Astronomy Program, Department of Physics & Astronomy, Seoul National University, Seoul 08826, Republic of Korea

[2]Korea Astronomy and Space Science Institute, Daejeon 305-348, Republic of Korea and

[3]Department of Astronomy and Space Science, Chungnam National University, Daejeon 305-764, Republic of Korea

Accepted for publication in the ApJ

ABSTRACT

A fraction of early-type dwarf galaxies in the Virgo cluster have a disk component and even possess disk features such as bar, lens, and spiral arms. In this study, we construct fifteen galaxy models that resemble VCC856, considered to be an infalling progenitor of disk dwarf galaxies, within observational error ranges, and use N-body simulations to study their long-term dynamical evolution in isolation as well as the formation of bar in them. We find that dwarf disk galaxies readily form bars unless they have an excessively concentrated halo or a hot disk. This suggests that infalling dwarf disk galaxies are intrinsically unstable to bar formation, even without any external perturbation, accounting for a population of barred dwarf galaxies in the outskirts of the Virgo cluster. The bars form earlier and stronger in galaxies with a lower fraction of counter-streaming motions, lower halo concentration, lower velocity anisotropy, and thinner disk. Similarly to normal disk galaxies, dwarf disk galaxies also undergo recurrent buckling instabilities. The first buckling instability tends to shorten the bar and to thicken the disk, and drives a dynamical transition in the bar pattern speed as well as mass inflow rate. In nine models, the bars regrow after the mild first buckling instability due to the efficient transfer of disk angular momentum to the halo, and are subject to recurrent buckling instabilities to turn into X-shaped bulges.

Keywords: galaxies: dwarf – galaxies: kinematics and dynamics – galaxies: bulges – galaxies: clusters: general – galaxies: evolution – galaxies: structure – instabilities – methods: numerical